Molecular-Sieving Capabilities of Mesoporous Carbon Membranes

ARTICLE *in* THE JOURNAL OF PHYSICAL CHEMISTRY B · AUGUST 2008

Impact Factor: 3.3 · DOI: 10.1021/jp8006427 · Source: PubMed

6 AUTHORS, INCLUDING:

Xiqing Wang
Nanotek Instruments, Inc.
55 PUBLICATIONS **2,246** CITATIONS
SEE PROFILE

Costas Tsouris
Oak Ridge National Laboratory
233 PUBLICATIONS **3,594** CITATIONS
SEE PROFILE

Molecular-Sieving Capabilities of Mesoporous Carbon Membranes

Chia-Hung Hou,[†,‡] Xiqing Wang,[‡] Chengdu Liang,[‡] Sotira Yiacoumi,[†] Costas Tsouris,[§] and Sheng Dai*[,‡]

School of Civil and Environmental Engineering, Georgia Institute of Technology, Atlanta, Georgia 30332-0373, Chemical Sciences Division, Oak Ridge National Laboratory, Oak Ridge, Tennessee 37831-6201, and, Nuclear Science and Technology Division, Oak Ridge National Laboratory, Oak Ridge, Tennessee 37831-6181

Received: January 18, 2008; Revised Manuscript Received: May 17, 2008

The size-sieving properties of a mesoporous carbon membrane were studied via molecular permeation and cyclic voltammetry experiments. Two phenomena, simple diffusion and electrochemically aided diffusion, were investigated. Molecular diffusion through the membrane was caused by a concentration gradient across the membrane and was facilitated by electrosorption of ions under an externally applied electric field. The diffusion of molecules transported through the membrane was characterized by the values of permeability and apparent diffusion coefficient in the membrane. Because larger molecules are more restricted in terms of penetrating the pores, the size-based selectivity of the mesoporous carbon membrane could be readily observed. For example, in the two-component permeation experiment, a high selectivity ($\alpha = 56.9$) of anilinium over Rhodamine B was found. It is inferred that the diffusive transport of the larger Rhodamine B molecules with a more extensive retardation comes from the competitive mechanism between the two kinds of molecules in accessing the pore. A series of voltammetric experiments involving a mesoporous carbon membrane immersed in various electrolytes with ions of different sizes allowed the observation of ion-exclusion phenomena. It was found that the size effect is significant for electrochemically aided diffusion and electrosorption processes. The number of cations inside the pores of the membrane decreases with increasing cation size. This phenomenon is due to the size-exclusion effect, which could be demonstrated by the values of electrical double-layer capacitance for sodium, magnesium, and tetrahexylammonium cations, at potentials ranging from negative values to the point of zero charge, corresponding to 86.7, 73.1, and 50.0 F/g, respectively. The findings of this work manifest that the relationship between the pore size and the dimensions of the molecules determines the transport and sorption behavior of nanoporous carbon materials.

1. Introduction

Carbon materials of porous structure such as activated carbon, carbon fiber, carbon aerogel, and graphite are ubiquitous and indispensable in various technologies. Because of their high surface area and unique physicochemical properties, porous carbons constitute very attractive materials for many applications, such as separation processes, water purification, catalysis support, and energy storage. When pore sizes approach molecular dimensions, activated carbons and carbon molecular sieves can provide selective separation of molecules via differences in their sorption capacity or diffusion rates.[1–4] In fact, the molecular-size effect is one of the critical factors for the performance of porous carbon materials.

The size-based selectivity of molecules transported through a membrane represents a possible separation mechanism within various chemical and biological systems.[5–11] For example, Jirage et al.[5] reported selective membranes containing an ensemble of gold nanotubes to selectively separate small molecules on the basis of molecular-sieving effects, in which transport selectivity increased as the inner diameter of the nanotubles decreased. Electrosorption, defined as the accumulation of ions next to a charged surface without triggering electrochemical reactions, is another promising application of porous carbon materials in energy storage and capacitive desalination.[12–14] In electrosorption processes, porous carbon materials can be considered as electrical double-layer capacitors (EDLCs), characterized via a double-layer capacitance at the interface of the carbon and the electrolyte.[15,16] A number of studies[3,17–20] have shown that porous carbon materials with very small pores exhibit limitations for molecule penetration, and thus, they do not contribute to the double-layer capacitance because of the molecular-sieving effect. Therefore, porous carbon materials could be potentially used to estimate effective ion dimensions of aqueous and organic electrolytes, as well as ionic liquids.[18,21,22]

The property of porous carbon materials that is indicative of their molecular-sieving capability is the corresponding pore-size distribution (PSD). The PSD affects not only the surface area available for sorption but also the accessibility of molecules.[15,20,23,24] According to the nomenclature of the International Union of Pure and Applied Chemistry (IUPAC), the pore size can be classified as micropores (pore diameter < 2 nm), mesopores (2 nm $<$ pore diameter < 50 nm), and macropores (pore diameter > 50 nm). Conventional porous carbon materials usually exhibit broad pore-size distributions, ranging from micropores to macropores, and the corresponding pores are randomly connected. The presence of micropores is an essential feature in the high specific surface area for porous carbon materials. However, there is a conflict between enhancing surface area of pores and improving the pore accessibility; micropores exhibit slow molecular motion

* Author to whom correspondence should be addressed. E-mail address: dais@ornl.gov.
[†] Georgia Institute of Technology.
[‡] Chemical Sciences Division, Oak Ridge National Laboratory.
[§] Nuclear Science and Technology Division, Oak Ridge National Laboratory.

10.1021/jp8006427 CCC: $40.75
Published on Web 07/01/2008

and low conductivity, and their porous structures collapse during high-temperature treatments.[15,16,19,25,26] In contrast, mesopores show a fast mass transfer rate of molecules.[15,16,26] Therefore, ordered mesoporous carbons, which have narrow pore-size distributions and less micropores present, are much desirable materials in numerous applications.[25] The relationship between the pore size of porous carbon materials and the molecular dimensions has a profound effect on the transport and sorption of molecules confined in a small space.

Recently, mesoporous carbon materials with ordered structures have been synthesized by us and other research groups using the self-assembly synthesis method through polymerization of phenolic resins in the presence of soft templates followed by carbonization.[27–34] The hydrogen bonding between soft templates and carbon precursors (i.e. phenolic resins) is the key to the successful self-assembly synthesis of highly ordered mesoporous carbons.[27,28] Pluronic triblock copolymers were used as structure-directing agents. Phenolic resins formed by polymerization of formaldehyde and phenols (e.g., phloroglucinol and resorcinol) can form multiple hydrogen bonding with the polyethylene chains of triblock copolymer. One of the unique features of the soft-templating method is the ease of control of different morphologies of mesoporous carbon materials, such as monoliths, films, fibers, micro/nanowires, and spheres.[28,35,36]

Although microporous carbon molecular sieve membranes have been well studied for gas separation,[37] the synthesis and studies in separation properties of mesoporous carbon membranes are very limited.[38,39] Herein, we report the preparation of mesoporous carbon membranes with well-defined porous structures by the soft-templating method and investigate their molecular-sieving properties. Two phenomena, simple diffusion and electrochemically aided diffusion and electrosorption, are investigated with a specific focus on size-exclusion effects. First, diffusion of different-sized molecules through the pores, caused by a concentration gradient, is studied to prove the size-sieving properties of the mesoporous carbon membranes. Second, diffusion and electrosorption experiments of different-size ionic species into the pores due to an applied electric field are conducted to investigate the ion size-exclusion effect in the double-layer region. The experimental results obtained in this work can provide a better understanding of the capabilities of these novel mesoporous carbon materials and contribute to assessing their potential applications, especially for separation technologies and energy storage.

2. Materials and Methods

2.1. Preparation and Characterization of Carbon Materials. Mesoporous carbon membranes were prepared via self-assembly of block copolymer and phenolic resin according to a procedure reported in our previous study.[28] Typically, 6.3 g of phloroglucinol (Aldrich) and 6.3 g of F127 ($EO_{106}PO_{70}EO_{106}$, Aldrich) were dissolved in 45 g of an ethanol−water mixture (10:9 in mass ratio) containing 0.5 g of concentrated HCl (Aldrich). An amount of 6.5 g of formaldehyde (37% in water, Sigma) was then added to the solution. The mixture was stirred at room temperature and turned cloudy after about 17 min, indicating the occurrence of phase separation. After stirring for another 13 min, the polymer-rich phase was separated out by centrifuge at 9500 rpm for 4 min. The polymer phase collected in the bottom of the centrifuge tube was redissolved in 10 g of ethanol. After removal of any air bubbles, the clear ethanolic solution of polymer was then loaded on a substrate via the tape-casting technique, giving a homogeneous and clear polymer film on the substrate. The film was dried in the air at room temperature overnight and subsequently cured in an oven at 80 °C for 24 h. The self-standing polymer film was detached from the substrate and cut into desired sizes. Carbonization was carried out in a tubular furnace under inert atmosphere (e.g., N_2) at 400 °C for 2 h with a heating ramp of 1 °C/min and then at 850 °C for another 2 h with a ramp of 5 °C/min from 400 °C. The nitrogen sorption isotherm of mesoporous carbon membrane was recorded on a Micromeritics Gemini 2375 analyzer at 77 K. The specific surface area was calculated using the Brunauer−Emmett−Teller (BET) method from the nitrogen adsorption data in the relative pressure range (P/P_0) of 0.05−0.30. The PSD plot was derived from the adsorption branch of the isotherm on the basis of the Barrett−Joyner−Halenda (BJH) method. Scanning electron microscope (SEM) images were taken on a Hitachi HD-2000 STEM microscope operating at 200 kV under SE mode.

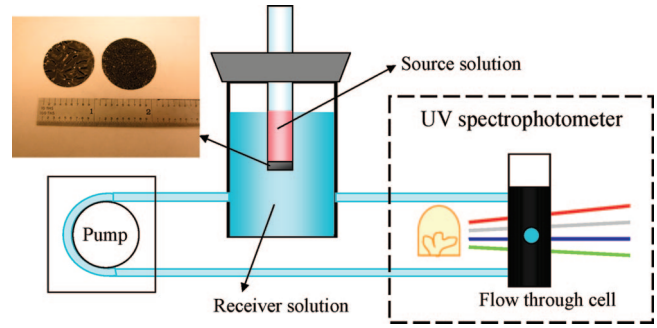

Figure 1. Schematic of the setup for permeation experiments with the carbon membrane. A UV−vis spectrophotometer was used to measure the concentration of the probe molecule in the receiver solution as a function of time. A photograph image reveals the size of our membranes synthesized for our experiments.

2.2. Permeation Experiments. The permeation experiments were carried out using a measuring cell as shown in Figure 1. The permeation cell consisted of the source and receiver solutions, which were separated by a mesoporous carbon membrane with a permeation area of 0.5 cm^2. Before any experiments were performed, the carbon membrane was immersed in deionized water to ensure proper wetting conditions. The source solution was an aqueous solution containing the probe species. The receiver solution initially contained deionized water. The volumes of source and receiver solutions were 0.8 and 16.8 cm^3, respectively. In each experiment, the receiver solution was continuously pumped through the flow cell installed in the circuiting line. The concentration of probe species in the receiver solution was measured in the flow-through cell as a change in spectroscopic absorbance using an ultraviolet−visible (UV−vis) spectrophotometer (Cary 5000, Varian Inc.). Calibration of the optical absorbance of the molecules was made by measuring the absorbance of a series of dilution solutions over a wide range of concentrations. For the permeation experiments, two test molecules, anilinium chloride (97%, Sigma-Aldrich, molecular weight 130) and Rhodamine B (95%, Sigma-Aldrich, molecular weight 479), were chosen to examine the effect of molecular dimension on the transport of species through the mesoporous carbon membrane. The reproducibility of the results was confirmed by repeating several permeation experiments under identical conditions. All experiments were carried out at room temperature.

2.3. Electrochemical Measurements: Cyclic Voltammetry. Cyclic voltammetry experiments were performed using a CH Instruments model 604B electrochemical analyzer in conjunction with a Bioanalytical Systems model C-2 electrochemical cell. A three-electrode system was used for these experiments; the

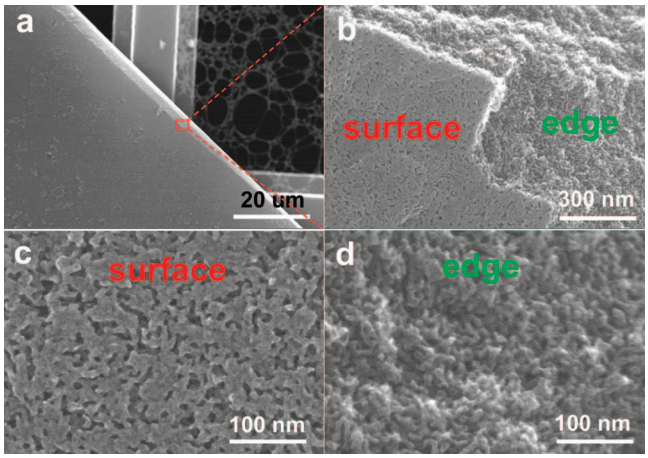

Figure 2. SEM images of a mesoporous carbon membrane at low (a) and high (b, c, d) magnifications.

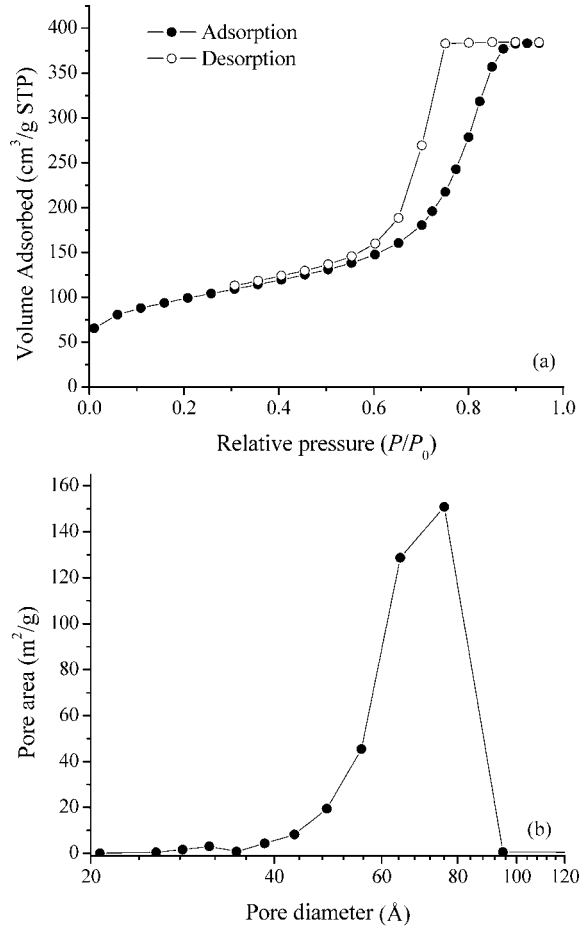

Figure 3. (a) Nitrogen adsorption/desorption isotherms and (b) pore-size-distribution plot of the mesoporous carbon membrane (STP, standard temperature and pressure).

working electrode was a small piece of mesoporus carbon membrane clipped to a platinum wire in the aqueous solution. The counter electrode was a large piece of commerical carbon paper, and the reference electrode was an Ag/AgCl electrode immersed in a 3 M NaCl electrolyte solution (Bioanalytical Systems). The electric current, obtained in the original experimental data, was normalized as the specific capacitance in Farads per gram of carbon material and per unit scan rate. The range of potentials applied to the system was +0.6 to −0.4 V within a pure electrical double layer (EDL) window where faradaic reactions do not take place. Thus, the specific capacitance may be basically attributed to the EDL capacitance as a result of electrosorption of ions.[15,16] Aqueous solutions used in cyclic voltammetry experiments were prepared using deionized water (Millipore) and sodium chloride (NaCl, >99%), magnesium chloride ($MgCl_2$, 98%) and tetrahexylammonium chloride (THACl, 96%) obtained from Sigma-Aldrich.

3. Results and Discussion

3.1. Characterization of the Carbon Membrane. Figure 2 shows high-resolution SEM images of mesoporous carbon membranes, clearly revealing the well-defined mesoporosity both on the surface and on the edge (body). A disordered structure was observed and also confirmed by a low-angle XRD pattern (see Supporting Information). As seen in Figure 3, mesoporous carbon membranes exhibit a typical type IV nitrogen adsorption/desorption isotherm with a pronounced uptake in the relative pressure range (P/P_0) of 0.6−0.85 and a narrow PSD centered at about 7.2 nm. The BET surface area of the carbon membrane was calculated to be 332.1 m^2/g. The contribution of micropores to the surface area was 78.1 m^2/g, and a large portion of the pores was in the mesoporous range 5−9 nm. The well-defined mesoporosity is believed to be due to the self-assembly of phenolic resins and Pluronic block copolymers into organized structures. On the contrary, polyimide derived mesoporous carbon membranes using poly(ethylene glycol) as a template exhibited a very broad PSD.[38]

3.2. Molecular-Sieving Effect. Figure 4a presents the absorbance of UV spectra for the single-component permeation of 5 mM anilinium chloride solution transported through the membrane to a receiver solution of deionized water. The absorbance at a wavelength of 230 nm was used for measuring the anilinium concentration in the receiver solution. Neutral aniline absorbs light at a wavelength of 280 nm.[40] The absorbance changes at 230 and 280 nm indicated that anilinium is the predominant species in the solution. Moreover, the pH values were measured in the source and receiver solutions to ensure that the proportion of neutral aniline and anilinium cation was kept constant during the experiment. The chemical structure of anilinium is also shown in Figure 4a. As shown in Figure 4b, the experimental data are represented as plots of moles of the probe substance transported per unit area (in square meters) of membrane vs permeation time. Because the transport of anilinium through the membrane is a result of the concentration gradient between the source and receiver solutions, the concentration initially increases linearly as a function of time and finally reaches a plateau. Figure 5 shows the data in the single-component experiment for a source solution of 5 mM Rhodamine B and a receiver solution of deionized water. In the beginning of the experiment, the absorbance change of Rhodamine B was insignificant in the receiver solution. After a retention time of approximate 180 min, the Rhodamine B molecules penetrated through the membrane and the linear increase of concentration in the receiver solution was observed. This time lag for the transport of Rhodamine B through the membrane, before the steady-state concentration gradient could be achieved, may result from the combination of sorption of Rhodamine B onto the pore walls and slow penetration of the molecules into the membrane. It is evident that the molecular-transport rate decreases as the size of molecule increases.[5] Rhodamine B molecules have larger size than anilinium molecules; thus there are more restrictions for Rhodamine B molecules in penetrating the pores, leading to slow permeability.

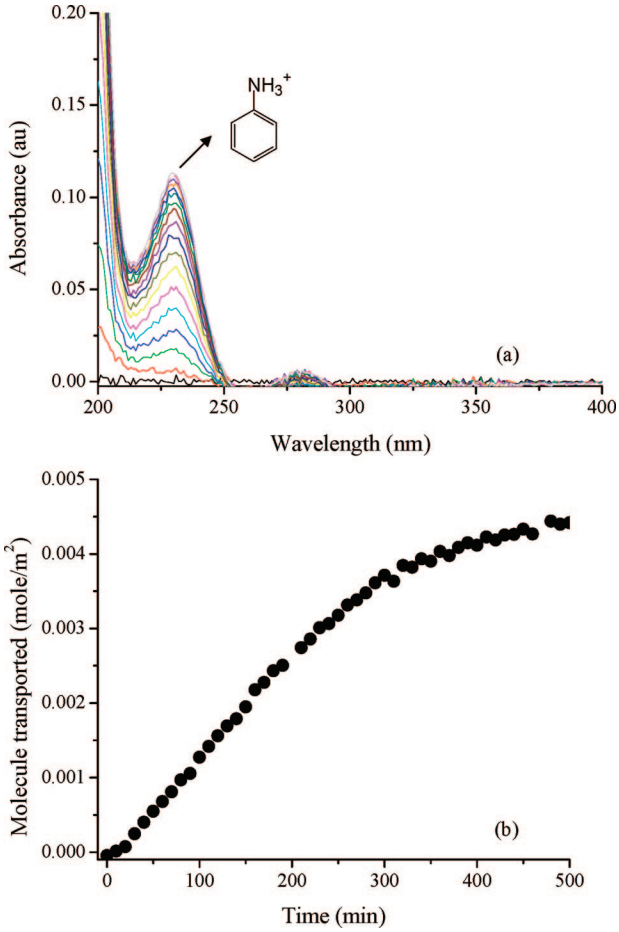

Figure 4. Single-component experiment for a source solution of 5 mM anilinium chloride transported through the mesoporous carbon membrane. (a) Absorbance spectra of anilinium recorded at the interval of 30 min. (b) Concentration of anilinium in the receiver solution as a function of time.

In the present work, the characterization of the diffusion of molecules through the membrane in terms of a concentration-gradient driven process can be generally described by Fick's law.[41,42] In the beginning of the permeation experiments, the concentration changes in both the receiver solution and the source solution were small, and the concentration difference between the two solutions was considered constant. One can calculate the steady-state flux through the membrane obtained from the slope of the straight line shown in Figures 4b and 5b. It was found that the observed diffusion data present a linear dependence that obeys Fick's law. Therefore, when steady state is reached, the membrane permeability coefficient of component i, $P_{i,\mathrm{m}}$, can be estimated in terms of the steady-sate flux (J_i) and the concentration gradient normalized by the membrane thickness (L), as follows

$$P_{i,\mathrm{m}} = -J_i \frac{L}{C_{i,1} - C_{i,2}} \tag{1}$$

where $C_{i,1}$ and $C_{i,2}$ are the concentrations of component i in the source solution and the receiver solution at the other side of the membrane, respectively. In the analysis of the time lag t_{lag}, the apparent diffusion coefficient ($D_{i,\mathrm{app}}$) can be determined by using the equation[43]

$$D_{i,\mathrm{app}} = \frac{L^2}{6t_{\mathrm{lag}}} \tag{2}$$

The membrane permeability and the apparent diffusion coefficient can be further connected by the relation[41,43]

$$P_i = K_i D_{i,\mathrm{app}} \tag{3}$$

where K_i is a partition coefficient of component i (a ratio between membrane and external solution concentrations). It is noted that the diffusion parameters (i.e., $P_{i,\mathrm{m}}$ and $D_{i,\mathrm{app}}$) were used to characterize the diffusion permeability of the molecules transported through the membrane as the means to demonstrate the size-sieving properties of the carbon membrane. For example, the apparent diffusion coefficient could be a complex average of the true local diffusion coefficients in the membrane.[43] From the experimental data, the membrane permeability coefficients ($P_{i,\mathrm{m}}$) of anilinium and Rhodamine B were 1.38×10^{-8} and 5.39×10^{-10} cm^2/s, respectively. In addition, the apparent diffusion coefficient ($D_{i,\mathrm{app}}$) obtained from the time lag was calculated as 1.39×10^{-10} cm^2/s for Rhodamine B, corresponding to a value of $K_i = 3.9$. Assuming the partition coefficient of anilinium was equal to 1.0 led to an estimated lag time of less than 2 min. This time can explain that no apparent time lag was observed for the transport of anilinium through the membrane. In summary, the results indicate that the size-exclusion effect decreases the transport rate of Rhodamine B, much more than that of anilinium. Due to confinement, the diffusion rate of molecules is greatly affected by their size.

The diffusivity of molecule i in bulk solution (water) can be characterized by the diffusion coefficient, $D_{i,0}$, which can be approximated using the Stokes−Einstein equation[42]

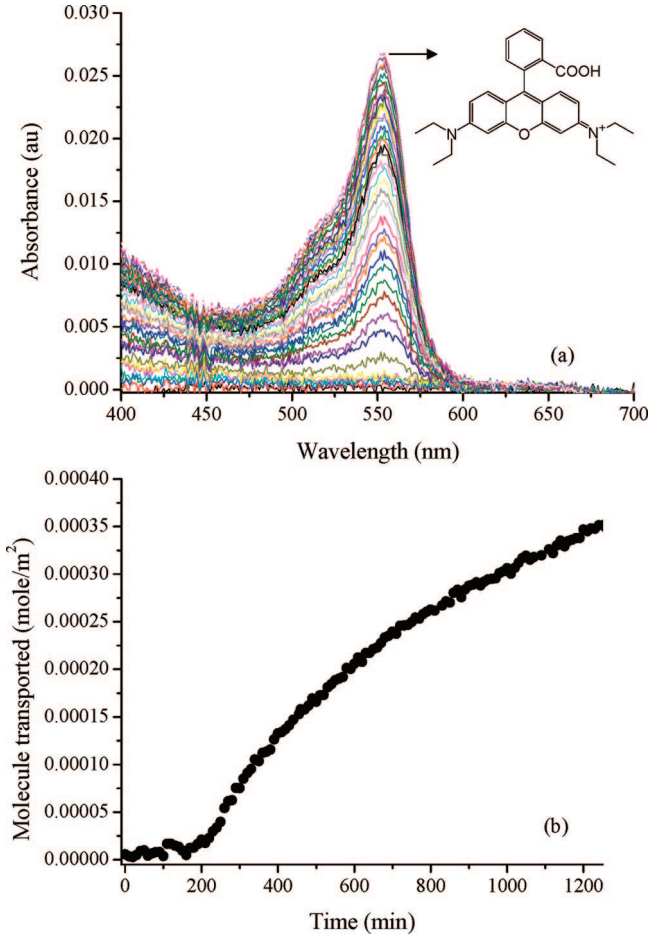

Figure 5. Single-component experiment for a source solution of 5 mM Rhodamine B transported through mesoporous carbon membrane. (a) Absorbance spectra of Rhodamine B recorded at the interval of 30 min. (b) Concentration of Rhodamine B in the receiver solution as a function of time.

$$D_{i,0} = \frac{kT}{6\pi\eta r} \quad (4)$$

where k is the Boltzmann constant, T is the Kelvin temperature, η is the viscosity of water, and r is the radius of the diffusing molecule. When the radii of anilinium and Rhodamine B are taken as 2.9 and 8.0 Å, respectively, the diffusion coefficients for anilinium and Rhodamine B in bulk solution are 8.45×10^{-6} and 3.06×10^{-6} cm^2/s, respectively. In the experimental data, the estimated apparent diffusion coefficient of anilinium was about 3 orders of magnitude smaller than that in bulk solution, and the apparent diffusion coefficient of Rhodamine B was 5 orders of magnitude smaller than that in bulk solution.

The diffusive-transport selectivity of the membrane (α) can be defined by the ratio of the membrane permeability of anilinium to that of Rhodamine B. The selectivity toward transport of anilinium within the mesoporous carbon membrane ($\alpha = 25.6$) was significantly enhanced from that in bulk solution (i.e., the ratio of their bulk diffusion coefficients is only 2.8). The experimental results demonstrate that the mesoporous carbon-based membrane has the ability to separate the molecules via molecular-size selectivity.

According to the Renkin equation, the diffusion coefficient of component i confined to a pore, $D_{i,\text{pore}}$, is determined by the ratio of the molecular radius (a) to the pore radius (r)

$$\frac{D_{i,\text{pore}}}{D_{i,0}} = \left(1 - \frac{a}{r}\right)^2\left[1 - 2.104\frac{a}{r} + 2.09\left(\frac{a}{r}\right)^3 - 0.95\left(\frac{a}{r}\right)^5\right] \quad (5)$$

Theoretically, the restriction factor ($D_{i,\text{pore}}/D_{i,0}$) could be used to predict the restriction to molecular diffusion through membranes, which is a result of the combination of steric hindrance at the entrance to the pores and frictional resistance within the pores.[44] When one takes into account the radius of anilinium as 2.9 Å, the restriction factors are 0.59, 0.70, and 0.78 for the pore sizes of 5, 7, and 10 nm, respectively. The values of 0.18, 0.32, and 0.47 represent the theoretical restriction factors of Rhodamine B with pore sizes of 5, 7, and 10 nm. The theoretically calculated values of the ratio of the diffusion coefficients ($D_{\text{anilinium,pore}}/D_{\text{RhodamineB,pore}}$) of the two molecules are 9.0, 6.0, and 4.6 for the 5, 7, and 10 nm mesopores, respectively. However, a selectivity coefficient $\alpha = 25.6$ was obtained from the permeation experiments. Although the theoretical prediction clearly underestimates the membrane selectivity obtained by the permeation experiments, it provides consistent description of permeability characteristics. The difference between experimental and theoretical values may be caused from the simplifications introduced in the Renkin equation by ignoring the interaction between molecule and pore surface, the nonparallel alignment and nonuniformity of pores, and the irregular pore connections which decrease molecular motion.

Figure 6 illustrates the absorbance changes and the molecule-transported histories for anilinium and Rhodamine B in the receiver solution during two-component permeation experiments. As expected, the anilinium molecules of smaller size can easily pass through the membrane with low pore restriction. On the contrary, larger Rhodamine B molecules, with a slow transport rate, cannot be detected by the UV−vis instrument until a permeation time of 500 min. When the results of the two-component experiments are compared with the results of single-component experiments, one can note that the membrane permeability for anilinium increases slightly to 1.57×10^{-8} cm^2/s. On the other hand, the permeability of rhodamine B in the two-component mixture (i.e., $P_{i,\text{m}} = 2.76 \times 10^{-10}$ cm^2/s) is much slower than that in the single-component solution. The

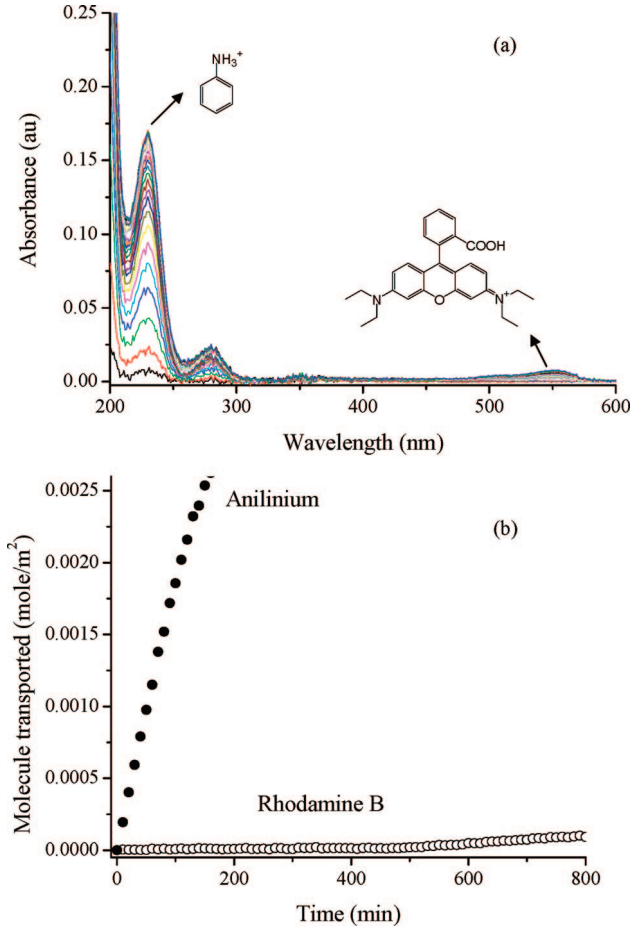

Figure 6. Two-component experiment for a source solution of the mixture of 5 mM anilinium chloride and 5 mM Rhodamine B transported through mesoporous carbon membrane. (a) Absorbance spectra of anilinium and Rhodamine B recorded at the interval of 30 min. (b) Concentration of test molecules in the receiver solution as a function of time.

carbon membrane shows greater selectivity toward the small anilinium molecules over the large Rhodamine B molecules, i.e., a larger selectivity coefficient of $\alpha = 56.9$ is obtained. It is also noted that the time lag of Rhodamine B extends from 180 min, in the single-component experiments, to 500 min, in the two-component experiments. Also, the apparent diffusion coefficient and the partition coefficient are 5.21×10^{-11} cm^2/s and 5.3, respectively. These data suggest that these two molecules not only interact with the pore walls of the membrane but possibly also compete with each other. The transport of large rhodamine B molecules through the membrane is limited by the presence of small anilinium molecules. When both anilinium and Rhodamine B exist in the solution, they compete with each other for access into the pores. Initially, the pores are only accessible to the smaller anilinium molecules that have "size affinity", while at the same time, larger Rhodamine B molecules have higher restriction at the entrance of the pores. When the concentration gradient of anilinium decreases sufficiently, the driving force for transport of Rhodamine B is able to overcome the competitive size effect, allowing this species to pass through the pores. According to the size-based selectivity, the mesoporous carbon membrane can separate larger Rhodamine B molecules from smaller anilinium molecules in a mixture solution.

In general, diffusion due to concentration gradients is responsible for the movement of the permeate molecule from

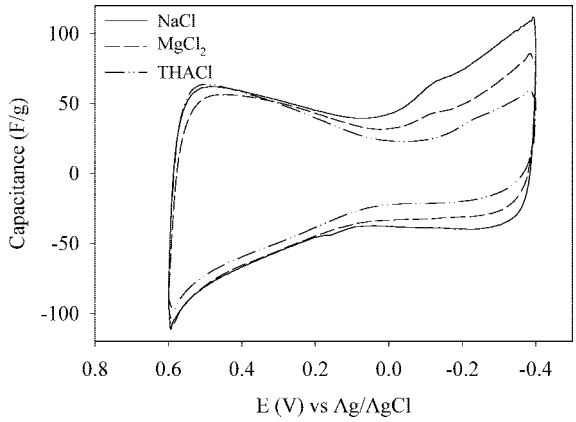

Figure 7. Cyclic voltammetry experiments with mesoporous carbon membrane immersed in various electrolyte solutions: 0.1 M NaCl, 0.05 M $MgCl_2$, and 0.1 M THACl. The data were obtained at a slow scan rate of 1 mV/s.

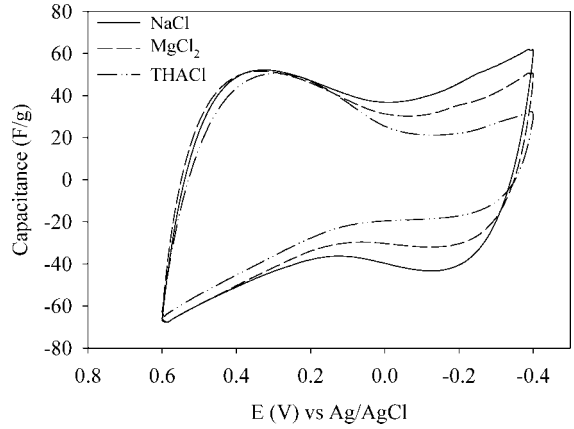

Figure 8. Cyclic voltammetry experiments with mesoporous carbon membrane immersed in various electrolyte solutions: 0.1 M NaCl, 0.05 M $MgCl_2$, and 0.1 M THACl. The data were obtained at a fast scan rate of 10 mV/s.

the source solution through the carbon membrane and into the receiver solution. Three factors can explain the mechanisms behind the retardation of diffusive transport of larger molecules within pores. First, the steric hindrance effect plays a determining role in the molecular accessibility at the entrance of pores.[45] Because the accessible cross-sectional area of pores decreases with increasing molecular size, there is higher restriction for a larger molecule to enter the pores. Second, the motion of a molecule through a small pore is significantly affected by the interaction in terms of friction resistance between the molecule and the pore surfaces.[6,45] Finally, a larger molecule with associated large exclusion volume from the pore wall decreases the average concentration inside the pore and reduces the average flux density.[46] Furthermore, when dealing with a mixture of species, a competitive behavior between molecules that have different sizes can be observed. Because of the confinement effect, the transport of larger molecules may be impeded by the transport of smaller molecules, leading to a more extensive retardation during the permeation process.

3.3. Ion-Size Effect. The investigation of the ion-size effect on EDL formation during electrosorption by the mesoporous carbon membrane was carried out using cyclic voltammetry experiments. Figures 7 and 8 present the cyclic voltammograms of the mesoporous carbon membranes in various electrolyte solutions using a slow scan rate (1 mV/s) and a fast scan rate (10 mV/s). The electrolyte solutions studied in comparative series were sodium chloride, magnesium chloride, and tetrahexylammonium chloride. One should note that the electrolyte solutions contained the same amount of chloride anions and, therefore, had the same charge capacity in each experiment.

The point of zero charge (pzc) is the value of the electrical potential at which the surface charge density is zero. Previous studies have shown that the specific capacitance at a slow scan rate goes through a minimum around the point of zero charge (pzc) for both positive and negative scans.[16] As shown in Figure 7, the pzc of the mesoporous carbon membrane in a 0.1 M sodium chloride solution can be estimated as 0.06 V (vs. Ag/AgCl in 3 M NaCl). When a potential range is chosen on either side of the pzc, electrosorption of counterions that have an opposite charge to that of the charged surface takes place in the EDL, resulting from the electrostatic interactions of ionic species and the charged surface. For example, Figure 7 shows that the cyclic voltammogram of NaCl exhibits a rectangular shape of the curve with increasing capacitance toward positive and negative potentials. Because of their similar hydrated ion size of 4.25 Å, the sodium cation (Na^+) and chloride anion (Cl^-) have a symmetric response during the electrosorption process.[18,20] At negative potentials with respect to the pzc, the electrosorption of Na^+ cations dominates the EDL formation to neutralize the surface charge. At the same time, Cl^- anions are excluded from the charged pores. On the other hand, Cl^- anions provide the major contribution toward electroneutrality within the EDL at positive potentials with respect to the pzc.

For a magnesium-chloride electrolyte solution, the ion-size effect of the mesoporous carbon membrane on the voltammetric behavior can be observed in Figures 7 and 8. For example, a comparison of cyclic voltammograms in 0.1 M NaCl and 0.05 M $MgCl_2$ aqueous solutions at a slow scan rate (1 mV/s) indicates that the capacitance of magnesium ion (Mg^{2+}) drops to 73.1 F/g at the potential of −0.4 V, which is only 83% of the capacitance of Na^+ ion. On the other hand, Cl^- ions present in these two solutions have the same magnitude of capacitance at the potential positive to the pzc. Because the concentrations selected in the experiments ensured that the Mg^{2+} and Na^+ cations provided the same charge capacity in each system, the EDL capacitance was expected to be independent of ion charge. Therefore, the observed loss of the double-layer capacitance can be mainly attributed to the size-exclusion effect of Mg^{2+} ions, which have a larger hydrated diameter of 8.0 Å, by the micropores of the carbon membrane. This result, furthermore, implied the successful development of EDL in the mesoporous region for large hydrated cations.

The voltammetric behavior of tetrahexylammonium ion (THA^+), which has tetraalkyl chains of about 8.6 Å radius, can further demonstrate the size effect on ion electrosorption. It can be seen that the cyclic voltammogram of tetrahexylammonium chloride shows an asymmetric response at the potential window between −0.4 and +0.6 V. As shown in Figure 7, the capacitance value decreases from 88.5 F/g for Cl^- anion to 50.0 F/g for THA^+ cation. This considerable loss (44%) of double-layer capacitance may result from the poor micropore accessibility for larger THA^+ ions. Moreover, an increase in ionic dimension results in a decrease of double-layer capacitance. For instance, when using a slow scan rate (Figure 7), the values of the capacitance measured at −0.4 V for Na^+, Mg^{2+}, and THA^+ cations are 86.7, 73.1, and 50.0 F/g, respectively. The explanation is that larger ions have larger limitations in terms of pore accessibility and tend to be excluded from the micropores, and at the same time, the density of ion accumulation inside the charged mesopores decreases with increasing ion size. Thus,

the mesoporous carbon membrane exhibits significant ion-size properties for ion electrosorption, which is affected by the size of ionic species involved in the EDL formation.

Overall, the electrosorption behavior of porous carbon materials depends on two factors: (i) mass transfer rate of ions to access the pores, and (ii) concentration of ions inside the pores at equilibrium with bulk solution.[15] As known from our previous studies,[15,16] mesopores are much easily and rapidly penetrated by ions, leading to good electrochemical accessibility. Therefore, the equilibrium state in mesopores can be reached at a slow scan rate (e.g., 1 mV/s), and the concentration of ions inside the pores will be the factor determining the capacitance measured in this experiment. When the pore size and the dimension of ionic species are comparable, the confinement effect becomes important and affects the concentration and distribution of ions inside a charged pore. This phenomenon is much related to the EDL formation, which is highly dependent on the characteristics of the ionic species present, such as ion charge and size. Due to the difference in ion charge, exclusion of co-ion from charged pores can be expected, while, at the same time, counterions become the predominating species contributing toward electroneutrality in the EDL. However, when the size of the counterion is comparable to the size of the pores, the EDL formation becomes sensitive to the size of ionic species in the confinement space. EDL formation may be distorted by steric effects because larger ions associated with a stronger size-exclusion effect cannot approach the pore surface as close as smaller ions. A larger ion-exclusion volume causes a decrease in the average concentration of ions in the charged pores. This feature explains the asymmetric curves obtained in cyclic voltammetry experiments when the ion-size effect occurs. The selectivity of ion electrosorption of mesoporous carbon could be achieved according to the affinity of ions of smaller size.

4. Conclusions

The present work demonstrates the molecular size-based sieving effect of mesoporous carbon membranes on molecules transported through the pores. The relationship between the pore size and the molecule size plays an extremely important role in the determination of transport and sorption behavior of mesoporous carbon membranes in aqueous solutions. One of the consequences is that molecular transport rates through a membrane, induced by a concentration gradient, can be decreased by the molecule-size effect. The restriction to penetrate the pore increases with increasing molecule size, and at the same time, the average concentration of molecules in the pore solution can be further reduced by their larger exclusion volume. When dealing with a mixture of solutions, molecules associated with different sizes present competition in accessing the pores, resulting in a more extensive retardation of larger molecules transported through the membrane.

When an external electric field is imposed, the ion-size effect on electrosorption of ions by the mesoporous carbon membrane is observed. Then ions can develop a double layer in the region of mesopores, and the properties of the ions determine the double-layer capacitance. Although symmetry in electrosorption of cations and anions takes place for small, symmetric electrolytes, for asymmetric electrolytes involving unequal ion size, ions of larger size have more distance of closest approach[47] to pore surface. Hence, larger ions are more easily excluded from the charged pores, resulting in asymmetric electrosorption behavior. This also suggests that ion accumulation in a charged pore, in which EDL forms, can determine the pore occupancy. As a result, the density of ions inside the pores decreases with increasing ion size. This observation is important because it plays a central role in ion selectivity. Membrane selectively allows the permeation of smaller ions with their size affinity. Selective separation of ions of different sizes may be achieved via the application of an external electric field on mesoporous membranes.

Consequently, the size-exclusion effect is one of the most important properties to be considered when dealing with the physical chemistry of porous materials in aqueous solutions and their possible applications in separation processes. The findings of this work can provide fundamental knowledge for the utilization of nanoporous carbon materials in separation processes, energy storage, or removal of contaminant from aqueous solutions.

Acknowledgment. This work was conducted at the Oak Ridge National Laboratory and supported by the Division of Chemical Sciences, Office of Basic Energy Sciences, U.S. Department of Energy, under contract No. DE-AC05-00OR22725 with UT-Battelle, LLC. This research was supported in part by an appointment for X.W. to the Oak Ridge National Laboratory Postdoctoral Research Associates Program, administered jointly by the Oak Ridge Institute for Science and Education and Oak Ridge National Laboratory. A portion of this research was conducted at the Center for Nanophase Materials Sciences, which is sponsored at Oak Ridge National Laboratory by the Division of Scientific User Facilities, U.S. Department of Energy. Partial support was also provided by the National Science Foundation, under Grant No. CBET-0651683.

Supporting Information Available: Low-angle XRD pattern of mesoporous carbon membrane. This material is available free of charge via the Internet at http://pubs.acs.org.

References and Notes

(1) Karanfil, T.; Dastgheib, S. A.; Mauldin, D. *Environ. Sci. Technol.* **2006**, *40*, 1321.
(2) Koresh, J.; Soffer, A. *J. Chem. Soc., Faraday Trans. 1* **1980**, *76*, 2457.
(3) Koresh, J.; Soffer, A. *J. Electroanal. Chem.* **1983**, *147*, 223.
(4) Koresh, J. E.; Soffer, A. *Sep. Sci. Technol.* **1987**, *22*, 973.
(5) Jirage, K. B.; Hulteen, J. C.; Martin, C. R. *Science* **1997**, *278*, 655.
(6) Martin, C. R.; Nishizawa, M.; Jirage, K.; Kang, M. *J. Phys. Chem. B* **2001**, *105*, 1925.
(7) Wirtz, M.; Parker, M.; Kobayashi, Y.; Martin, C. R. *Chem. Rec.* **2002**, *2*, 259.
(8) Yu, S. F.; Lee, S. B.; Kang, M.; Martin, C. R. *Nano Lett.* **2001**, *1*, 495.
(9) Snyder, M. A.; Tsapatsis, M. *Angew. Chem., Int. Ed.* **2007**, *46*, 7560.
(10) Yamaguchi, A.; Uejo, F.; Yoda, T.; Uchida, T.; Tanamura, Y.; Yamashita, T.; Teramae, N. *Nat. Mater.* **2004**, *3*, 337.
(11) Li, S.; Wang, X.; Beving, D.; Chen, Z. W.; Yan, Y. S. *J. Am. Chem. Soc.* **2004**, *126*, 4122.
(12) Farmer, J. C.; Fix, D. V.; Mack, G. V.; Pekala, R. W.; Poco, J. F. *J. Electrochem. Soc.* **1996**, *143*, 159.
(13) Frackowiak, E.; Beguin, F. *Carbon* **2001**, *39*, 937.
(14) Ying, T. Y.; Yang, K. L.; Yiacoumi, S.; Tsouris, C. *J. Colloid Interface Sci.* **2002**, *250*, 18.
(15) Hou, C. H.; Liang, C. D.; Yiacoumi, S.; Dai, S.; Tsouris, C. *J. Colloid Interface Sci.* **2006**, *302*, 54.
(16) Yang, K. L.; Yiacoumi, S.; Tsouris, C. *J. Electroanal. Chem.* **2003**, *540*, 159.
(17) Barbieri, O.; Hahn, M.; Herzog, A.; Kotz, R. *Carbon* **2005**, *43*, 1303.
(18) Eliad, L.; Salitra, G.; Soffer, A.; Aurbach, D. *J. Phys. Chem. B* **2001**, *105*, 6880.
(19) Lin, C.; Ritter, J. A.; Popov, B. N. *J. Electrochem. Soc.* **1999**, *146*, 3639.
(20) Salitra, G.; Soffer, A.; Eliad, L.; Cohen, Y.; Aurbach, D. *J. Electrochem. Soc.* **2000**, *147*, 2486.

(21) Ania, C. O.; Pernak, J.; Stefaniak, F.; Raymundo-Pinero, E.; Beguin, F. *Carbon* **2006**, *44*, 3126.
(22) Eliad, L.; Pollak, E.; Levy, N.; Salitra, G.; Soffer, A.; Aurbach, D. *Appl. Phys. A-Mater. Sci. Proces.* **2006**, *82*, 607.
(23) Endo, M.; Maeda, T.; Takeda, T.; Kim, Y. J.; Koshiba, K.; Hara, H.; Dresselhaus, M. S. *J. Electrochem. Soc.* **2001**, *148*, A910.
(24) Raymundo-Pinero, E.; Kierzek, K.; Machnikowski, J.; Beguin, F. *Carbon* **2006**, *44*, 2498.
(25) Liang, C. D.; Li, Z. J.; Dai, S. *Angew. Chem., Int. Ed.* **2008**, *47*, 3696.
(26) Yoon, S.; Lee, J. W.; Hyeon, T.; Oh, S. M. *J. Electrochem. Soc.* **2000**, *147*, 2507.
(27) Liang, C. D.; Hong, K. L.; Guiochon, G. A.; Mays, J. W.; Dai, S. *Angew. Chem., Int. Ed.* **2004**, *43*, 5785.
(28) Liang, C. D.; Dai, S. *J. Am. Chem. Soc.* **2006**, *128*, 5316.
(29) Tanaka, S.; Nishiyama, N.; Egashira, Y.; Ueyama, K. *Chem. Commun.* **2005**, 2125.
(30) Meng, Y.; Gu, D.; Zhang, F. Q.; Shi, Y. F.; Yang, H. F.; Li, Z.; Yu, C. Z.; Tu, B.; Zhao, D. Y. *Angew. Chem., Int. Ed.* **2005**, *44*, 7053.
(31) Rodriguez, A. T.; Chen, M.; Chen, Z.; Brinker, C. J.; Fan, H. Y. *J. Am. Chem. Soc.* **2006**, *128*, 9276.
(32) Hu, Q. Y.; Kou, R.; Pang, J. B.; Ward, T. L.; Cai, M.; Yang, Z. Z.; Lu, Y. F.; Tang, J. *Chem. Commun.* **2007**, 601.
(33) Lu, Y. F. *Angew. Chem., Int. Ed.* **2006**, *45*, 7664.
(34) Wang, X. Q.; Liang, C. D.; Dai, S. *Langmuir*, 2008, DOI: 10.1021/la800529v, in press.
(35) Steinhart, M.; Liang, C. D.; Lynn, G. W.; Gosele, U.; Dai, S. *Chem. Mater.* **2007**, *19*, 2383.
(36) Yan, Y.; Zhang, F. Q.; Meng, Y.; Tu, B.; Zhao, D. Y. *Chem. Commun.* **2007**, 2867.
(37) Ismail, A. F.; David, L. I. B. *J. Membr. Sci.* **2001**, *193*, 1.
(38) Hatori, H.; Kobayashi, T.; Hanzawa, Y.; Yamada, Y.; Iimura, Y.; Kimura, T.; Shiraishi, M. *J. Appl. Polym. Sci.* **2001**, *79*, 836.
(39) Shah, T. N.; Foley, H. C.; Zydney, A. L. *J. Membr. Sci.* **2007**, *295*, 40.
(40) Katakura, K.; Inaba, M.; Toyama, K.; Ogumi, Z.; Takehara, Z. *J. Electrochem. Soc.* **1994**, *141*, 1827.
(41) Ho, W. S. W.; Sirkar, K. K. *Membrane Handbook*; Chapman & Hall: New York, 1992.
(42) Bird, R. B.; Stewart, W. E.; Lightfoot, E. N. *Transport Phenomena*; Wiley: New York, 2002.
(43) Rousseau, R. W. *Handbook of Separation Process Technology*; Wiley Interscience: New York, 1987.
(44) Renkin, E. M. *J. Gen. Physiol.* **1954**, *38*, 225.
(45) Kathawalla, I. A.; Anderson, J. L.; Lindsey, J. S. *Macromolecules* **1989**, *22*, 1215.
(46) Cervera, J.; Garcia-Morales, V.; Pellicer, J. *J. Phys. Chem. B* **2003**, *107*, 8300.
(47) Hou, C. H.; Taboada-Serrano, P.; Yiacoumi, S.; Tsouris, C. *J. Chem. Phys.* **2008**, *128*, 044705.

JP8006427